

INVESTIGATION OF THE REACTIONS $^{31}\text{P}(n, \gamma)^{32}\text{P}$ AND $^{32}\text{S}(n, \gamma)^{33}\text{S}$

G. VAN MIDDELKOOP and P. SPILLING †

Fysisch Laboratorium der Rijksuniversiteit, Utrecht, Nederland

Received 29 March 1965

Abstract: The γ radiation following capture of thermal neutrons in ^{31}P and ^{32}S was investigated with scintillation-spectrometer techniques. Measurements of single and coincidence spectra and of γ - γ angular correlations yield the following spins in ^{32}P : $J(0.52) = 0$, $J(1.32) = (2)$, $J(4.04) = 1$, $J(4.88) = 1$, $J(5.35) = 2$ and $J(5.78) = 1$. The spins of the 1.15 and 3.26 MeV levels are confirmed to be 1 and 2, respectively. The γ -ray decay of some lower levels is determined too.

In the ^{33}S nucleus a 1.44–7.20 MeV cascade is detected. The spin and parity of the intermediate level are $\frac{3}{2}^+$ or $\frac{5}{2}^+$. However, the existence of a level at about 1.4 MeV, expected on basis of a shell-model calculation, cannot be proved. In a sum-coincidence measurement a few other two-step cascades are detected.

E

NUCLEAR REACTIONS ^{31}P , $^{32}\text{S}(n, \gamma)$, $E = \text{thermal}$; measured γ , $\gamma\gamma$ -coin, $\gamma\gamma(\theta)$.
 ^{32}P , ^{33}S deduced levels, J , branching. Natural targets.

1. Introduction

Several accurate measurements of the energies of gamma-ray transitions following capture of thermal neutrons were done with magnetic Compton spectrometers ^{1–3}), pair spectrometers ⁴) and diffraction spectrometers ⁵). It often remains difficult to fit the observed gamma rays in the level scheme.

A useful tool for this purpose is the coincidence technique, which still must be performed, unfortunately, with NaI scintillation crystals, having a low-energy resolution. However, the sum-coincidence technique ⁶) opened, especially in the (n, γ) reaction, a new perspective. Angular correlation measurements, finally, make possible the determination of spins.

The reaction $^{31}\text{P}(n, \gamma)^{32}\text{P}$ has been studied with a magnetic pair spectrometer by Kinsey *et al.* ⁷) and by Bartholomew and Higgs ⁴), with a magnetic Compton spectrometer by Groshev *et al.* ¹) and with a two-crystal scintillation spectrometer by Braid ⁸). Manning and Bartholomew ⁹) studied this reaction with γ - γ coincidence and angular correlation methods; they found $J(3.26) = 2$ and $J(1.15) = 1$. Much of the decay scheme is still unknown. Parities of many levels and limitation on possible spin values are known from the $^{31}\text{P}(d, p)^{32}\text{P}$ reaction ^{10, 14}). The transition to the $E_x = 2.22$ MeV level shows a $l_n = 0+2$ orbital momentum mixture ¹⁰), corresponding to $J^\pi = 1^+$. The ground state and first excited state have $J^\pi = 1^+$ and 2^+ , respectively ¹⁴).

† On leave of absence from the University of Oslo, Blindern, Norway.

The reaction $^{32}\text{S}(n, \gamma)^{33}\text{S}$ has also been studied with the methods mentioned above ^{1, 4, 7-9}), the latter yielding $J(3.22) = \frac{3}{2}$ and $J(0.84) = \frac{1}{2}$, while Trumpy ¹¹) and Vervier ¹²) reported gamma circular polarization measurements, using polarized neutrons, yielding E1 character for the $C \rightarrow 3.22$ MeV transition and $J^\pi(3.22) = \frac{3}{2}^-$. A sum-coincidence measurement was done by Burmistrov ¹³) yielding two-step cascades through the 0.84, (1.97), 3.22, (4.05), (7.02) and 7.42 MeV levels. A compilation of the results in both reactions is given by Endt and Van der Leun ¹⁴).

The present investigation of the $^{31}\text{P}(n, \gamma)^{32}\text{P}$ reaction has been undertaken to get a better understanding of the decay scheme and to determine the spins of a number of odd-parity levels and of a few low-lying even-parity levels. The latter are of special interest in view of the recent shell model calculations by Glaudemans ¹⁵).

The $^{32}\text{S}(n, \gamma)^{33}\text{S}$ reaction was studied to investigate the possible existence of a level at approximately 1.4 MeV as predicted in ref. ¹⁵).

A short description of the apparatus is given in sect. 2. The experiments are described in sect. 3. In sect. 4 some results, especially the radiation strengths of E1 primaries, are investigated a little closer.

2. The Apparatus

A horizontal beam hole of the Dutch High Flux Reactor (20 MW thermal power) – of the Oak Ridge Material Testing Reactor type – in Petten is in use for the equipment to be described. This beam hole is a radial one. A beam emerging from such a beam hole is not directly suited for a thermal neutron capture experiment, because the fast neutron flux is of the same order as the thermal neutron flux, while the gamma-ray dose rate is about $10^4 \text{ R} \cdot \text{h}^{-1}$.

In order to provide a thermal neutron beam extensive use is made of single crystal filters as already proposed by others ^{16, 17}). Especially bismuth, quartz and beryllium crystals are well suited for this purpose. Because of its high density bismuth should be preferred for gamma ray shielding. However, it is impossible to make perfect single crystals of bismuth. Therefore a compromise is found in using four quartz crystals, each 9 cm long, and one 10 cm long bismuth crystal. The filter, positioned at about 3 m from the target, is at room temperature.

The filtered and collimated beam has a thermal [†] neutron flux of about $4 \times 10^6 \text{ cm}^{-2} \cdot \text{s}^{-1}$ at the target position, the fast neutron flux and the gamma ray dose rate being approximately $10^3 \text{ cm}^{-2} \cdot \text{s}^{-1}$ and $0.35 \text{ R} \cdot \text{h}^{-1}$, respectively. The beam diameter at the target position is approximately 2 cm. However, the high flux is only obtained in the inner part of 1 cm diam. which is equal to the target diameter. From the end of the collimator up to the beam catcher, a distance of about 1 m, the beam is surrounded by a “beam tube”, the target being positioned half-way in this tube. This tube consists of a teflon inner and an aluminium outer tube, whereas the 5 mm

[†] The neutron spectrum is distorted by the filter. The average neutron energy is less than the average thermal value.

space in between these tubes, is filled with ^6LiF powder over a length of 30 cm, from the target position 15 cm in both directions, while the rest contains B_4C . The transmission for thermal neutrons of the ^6LiF part is about 10^{-5} .

The two gamma ray detectors are $12.7\text{ cm} \times 12.7\text{ cm}$ NaI(Tl)-scintillation crystals mounted on 7.6 cm photomultiplier tubes (Philips XP 1031). Both detectors are heavily shielded against background radiation as seen in fig. 1, where the essentials of the equipment are shown. In front of each crystal a conical lead collimator with a conical hole limits the detection area to one half of the crystal front area. The axes of the detectors are perpendicular to the beam. One detector, the stationary counter or D1, has its axis fixed in the horizontal plane, the movable counter or D2 is able to move around the target from horizontal to vertical position. The movable counter is balanced around the axis of rotation by two counterweights, moving along the sides of the stationary counter. The distance of both counters to the target is adjustable, the maximum solid angle being 0.025 sr.

The electronics system is conventional. The coincidence circuit is of the "fast-slow" type. The signals from the anodes of the photomultiplier tubes are fed to fast transistor equalizers producing pulses for the fast coincidence circuit, having a time resolution $2\tau = 30\text{ ns}$. Both counters, the amplifiers included, are gain-stabilized¹⁸⁾, for which purpose a strong peak in the gamma spectrum is used. Two differential discriminators in parallel select pulses from D1. Their mixed outputs go to the slow coincidence unit having a resolving time $2\tau = 2\text{ }\mu\text{s}$. They also produce pulses for the routing system of an Intertechnique 400-channel analyser, receiving its input signals from D2 and its gate signals from the slow coincidence unit. Two different coincidence spectra can thus be recorded simultaneously in two subgroups of 200 channels. This double coincidence technique is often used to estimate the "background" in a coincidence spectrum; one window selects the photopeak pulses from a special gamma ray, while the second window, having the same width, selects pulses of slightly higher energy which might result from Compton scattering of higher energy gamma rays. For sum-coincidence measurements the output pulses of the two amplifiers, connected with D1 and D2, respectively, are added and the sum is detected by a differential discriminator.

In angular correlation measurements the angle of the movable counter is changed automatically according to a chosen set of angles. The counting time at each angle is defined by a preset number of pulses from a BF_3 counter monitoring the beam. The measured spectra are punched on paper tape. The spectra at equal angles are added channel by channel with the aid of a computer. It is found that the distortion in the angular correlation due to target excentricity, inhomogeneous beam and inhomogeneities in the target is not more than 0.01 in the A_2 coefficient, the angular correlation function W defined as $W(\theta) = 1 + A_2P_2(\cos \theta) + A_4P_4(\cos \theta)$, in which θ is the angle between the emitted coincident gamma rays. This is tested by measuring the angular correlation of the 7.80–0.84 MeV cascade in the reaction $^{32}\text{S}(\text{n}, \gamma)^{33}\text{S}$ through the 0.84 MeV level having $J = \frac{1}{2}$. All angular correlation measurements are done with

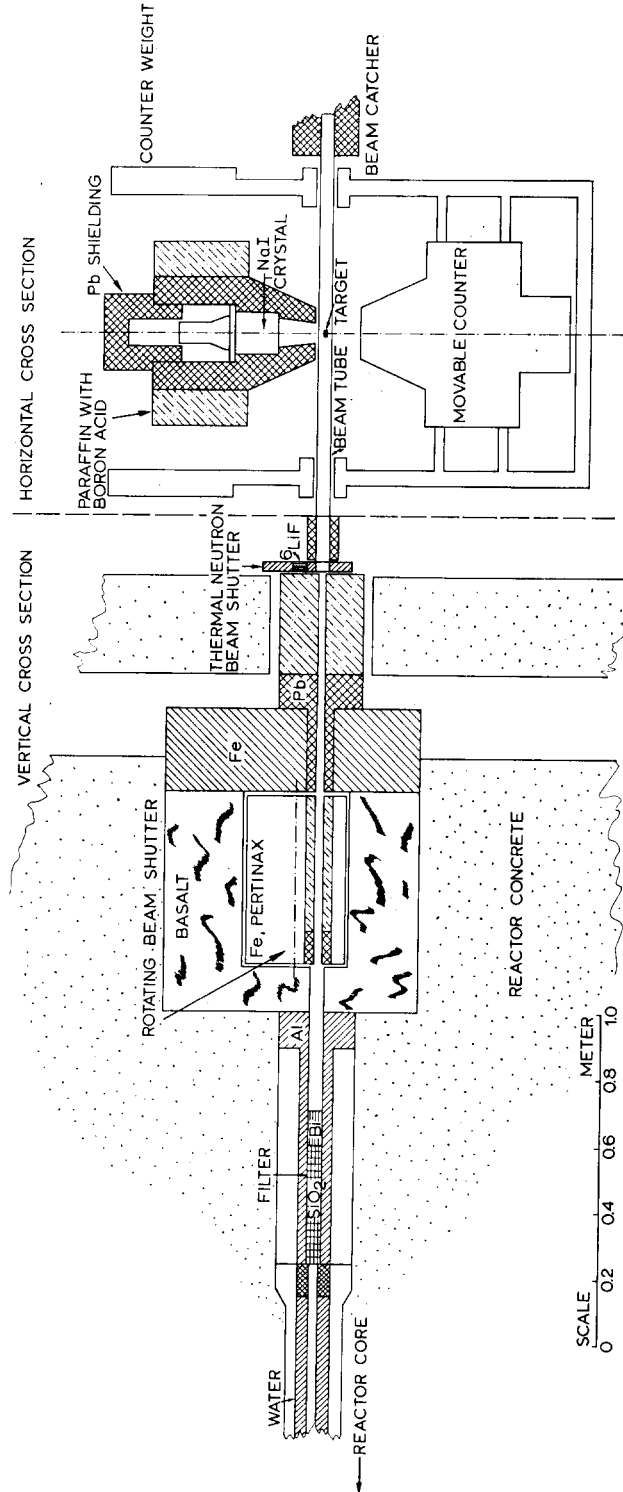


Fig. 1. Apparatus for studying (n, γ) reactions with coincidence and angular correlation techniques. Further description see text.

D1 and D2 having solid angles of 0.025 sr and 0.01 sr, respectively. Solid angle corrections were computed from the formulae given in ref. ¹⁹).

Pulse-height distributions for mono-energetic gamma rays were obtained using radioactive sources for gamma rays in the $E_\gamma = 0.5$ –3.0 MeV region. Transitions in the $E_\gamma = 3.0$ –12.0 MeV region were produced with (p, γ) reactions using the Utrecht 850 keV cascade generator.

Total detection efficiencies, as a function of gamma-ray energy and source-detector distance, were calculated with a computer, using a correction for the energy dependent transmission through the lead collimator.

3. Experimental Procedure and Results

3.1. THE REACTION $^{31}\text{P}(n, \gamma)^{32}\text{P}$

The thermal capture cross section and the average scattering cross section are ²⁰) 190 ± 10 mb and 5 ± 1 b, respectively. The reaction energy (neutron binding energy) is ¹⁴) 7.94 MeV.

The target consisted of 4.3 g of red phosphorus powder compressed in a thin-walled cylindrical teflon holder, having an inner diameter and length of 1.0 cm and 4.3 cm, respectively.

3.1.1. Decay scheme

The decay scheme, proposed mainly on basis of the present experiment, is given in fig. 2. It is divided in six parts noted a through f. The first four parts are derived from four sets of coincidence measurements (using sometimes results of angular correlation measurements) and from sum-coincidence measurements. Part e is determined from sum-coincidence measurements only, while f is taken from ref. ¹⁴). Use has been made also of a single spectrum measurement.

A single spectrum, corrected for background, is shown in fig. 3. The results of an analysis of the spectrum are listed in table 1. The lines used for energy calibration are marked (cal). The absolute intensities are calculated using the average (12 %) of the intensities of the 6.79 MeV gamma ray from refs. ^{1, 4}). In the analysis of the spectrum use has been made of preceding high-resolution measurements ^{4, 7}), especially for the three weak highest-energy lines, and of the coincidence measurements to be described below.

A sum-coincidence spectrum (I) with the sum channel at the binding energy is shown in fig. 4.

This spectrum was analysed up to an energy of 6 MeV with the aid of a computer, assuming Gaussian peak shapes. The number of peaks expected in a certain energy interval was given to the computer, while the positions, the widths and the relative intensities, using the detector-photopeak efficiencies, were calculated. The results are given in table 2. The intensities are derived from the known intensity of the 6.79 MeV gamma ray (12 %) and the branching in the decay of the 1.15 MeV level, see below.

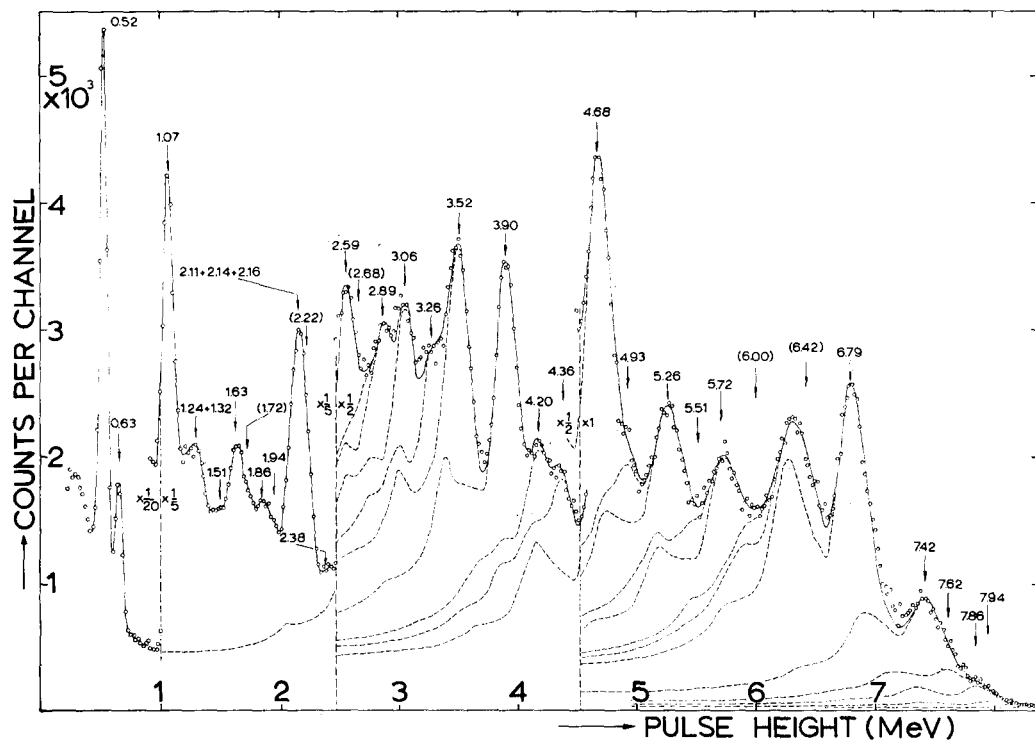


Fig. 3. Single spectrum of the $^{31}\text{P}(n, \gamma)^{32}\text{P}$ reaction, corrected for background. Detector solid angle 0.01 sr, counting time 15 min. The dotted lines show the pulse-height distribution for each γ ray.

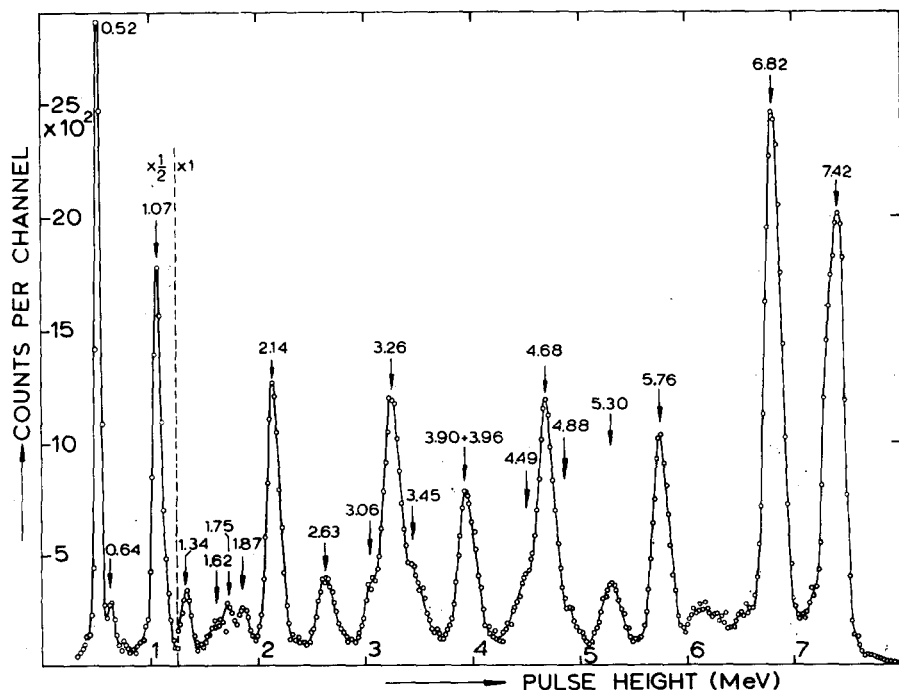


Fig. 4. Sum-coincidence spectrum of the $^{31}\text{P}(n, \gamma)^{32}\text{P}$ reaction. Sum channel 7.83-8.05 MeV, $\theta = 135^\circ$, counting time 72 h (the energies of the peaks at 5.30, 5.76 and 6.82 MeV are not correct, see text).

TABLE 1
Gamma rays observed in the single spectrum of the $^{31}\text{P}(n, \gamma)^{32}\text{P}$ reaction

E_γ (MeV)	Intensity (number of gamma rays per 100 captures)	E_γ (MeV)	Intensity (number of gamma rays per 100 captures)
7.94 ^{a)}	0.3 ^{a)}	2.86 \pm 0.03	4.6 \pm 0.9
7.85 ^{a)}	1.0 \pm 0.5	(2.68 \pm 0.03)	(1.4 \pm 0.7)
7.62 ^{a)}	1.4 \pm 0.6	2.56 \pm 0.02	4.2 \pm 0.6
7.42 \pm 0.02	4.4 \pm 0.7	2.38 \pm 0.03	2.6 \pm 0.9
6.79 (cal)	12 ^{b)}	(2.22 \pm 0.03)	(6.6 \pm 3.0)
(6.42 \pm 0.10)	(3.0 \pm 1.6)	2.16 \pm 0.02	5.0 \pm 1.2
(6.00 \pm 0.10)	(1.0 \pm 0.5)	2.14 \pm 0.02	5.0 \pm 1.2
5.71 \pm 0.03	4.4 \pm 0.7	2.11 \pm 0.02	5.3 \pm 1.2
5.51 \pm 0.06	1.4 \pm 0.5	1.95 \pm 0.03	2.3 \pm 0.9
5.26 \pm 0.02	4.9 \pm 0.7	1.85 \pm 0.02	2.9 \pm 0.8
4.92 \pm 0.04	1.9 \pm 0.5	(1.72 \pm 0.03)	(2.4 \pm 1.2)
4.67 \pm 0.02	11.2 \pm 1.3	1.63 \pm 0.02	4.4 \pm 1.0
4.38 \pm 0.04	5.5 \pm 1.1	1.50 \pm 0.03	1.6 \pm 0.8
4.18 \pm 0.03	3.9 \pm 1.2	(1.42 \pm 0.03)	1.2 \pm 0.6
3.90 (cal)	14.4 \pm 1.5	1.30 \pm 0.03	3.9 \pm 1.2
3.51 \pm 0.02	10.4 \pm 1.2	1.07 (cal)	9.6 \pm 1.0
3.27 \pm 0.03	4.7 \pm 0.8	0.64 \pm 0.01	9.6 \pm 1.0
3.05 \pm 0.02	5.5 \pm 0.6	0.52 \pm	
		annihilation radiation	

^{a)} From refs. ^{4,7}).

^{b)} Average intensity from refs. ^{1,4}). A 20 % error might exist in this value. This error is not included in the calculations.

TABLE 2
Two-step cascades observed in a sum-coincidence spectrum, gate on the capturing state energy, of the reaction $^{31}\text{P}(n, \gamma)^{32}\text{P}$

Cascade (MeV)	Intensity (number of two-step cascades per 100 captures)
0.52 (cal) — 7.42 (cal)	4.8 \pm 0.5
1.07 (cal) — 6.82 \pm 0.02 ^{a)}	6.2 ^s
1.34 \pm 0.02 — 6.6 ^{b)}	0.4 \pm 0.1
1.62 \pm 0.03 ^{c)} — 6.3 ^{b)}	0.3 \pm 0.1
1.75 \pm 0.03 — 6.2 ^{b)}	0.2 \pm 0.1
1.87 \pm 0.02 — 6.1 ^{b)}	0.4 \pm 0.1
2.15 \pm 0.02 — 5.76 \pm 0.02 ^{a)}	3.9 \pm 0.4
2.63 \pm 0.02 ^{c)} — 5.30 \pm 0.02 ^{a)}	1.4 \pm 0.2
3.05 \pm 0.02 — 4.87 \pm 0.03	0.8 \pm 0.2
3.25 \pm 0.02 ^{c)} — 4.68 \pm 0.02	4.7 \pm 0.7
3.44 \pm 0.03 ^{c)} — 4.52 \pm 0.03 ^{c)}	2.0 \pm 0.4
3.94 \pm 0.02 ^{d)} — 3.94 \pm 0.02 ^{d)}	1.8 \pm 0.2

^{a)} Energy too high. This gamma ray belongs to a cascade to the first excited state.

^{b)} Energy roughly calculated. It is uncertain whether the gamma ray proceeds to the ground state or to the first excited state (the line is unresolved in the spectrum).

^{c)} Possibly double.

^{d)} Combination of 3.90 and 3.96 MeV gamma rays forming one cascade.

It should be noted that ^{32}P has a ground-state doublet, the energy $^{14)}$ of the first excited state being 77 keV. This means that in the sum-coincidence measurement also two-step cascades ending on the 0.077 MeV level are included. In order to distinguish between these two types of cascades a second sum-coincidence measurement (II) was done with the sum channel at 7.86 MeV with the same width. Now the lines at 1.07 and 6.79 MeV, due to a cascade to the 0.077 MeV level $^{14)}$, are used for energy calibration. The assumption is made that energies of coincident gamma rays that add up to 7.94 ± 0.02 MeV in I and to ≥ 7.89 in II are members of a ground-state cascade, while, vice versa, energies adding up to ≤ 7.91 MeV in I and to 7.86 ± 0.02 MeV in II are members of a cascade to the first excited state. This is a powerful method since the (high-energy) peak energies are very sensitive to the sum-channel setting.

Ground-state cascades then are (in brackets the probable intermediate levels $^{14)}$ in MeV): 0.52–7.42 (0.52), 3.05–4.87 (4.88), 3.25–4.68 (3.26 and (4.66)) and 3.44–4.52 (3.45 and (4.41)) MeV. The cascades to the first excited state are: 1.07–6.79 (1.15), 2.13–5.73 (2.22, see below) and 3.93–3.93 (4.04, see below) MeV. The 5.30–2.63 MeV cascade in I or the 5.26–2.62 MeV cascade in II is a mixture of both types through the 2.66 and 5.35 MeV levels, see fig. 2.

TABLE 3
Gamma rays observed in the $^{31}\text{P}(\text{n}, \gamma)^{32}\text{P}$ reaction, using coincidence techniques

E_γ (MeV)	Intensity (number of gamma rays per 100 captures)	E_γ (MeV)	Intensity (number of gamma rays per 100 captures)
Gate: 6.66–6.87 MeV		Gates: 3.84–4.05 MeV and 4.12–4.33 MeV	
Coincident with 6.79 MeV		Coincident with 3.90 MeV	
1.15 \pm 0.02	0.7 \pm 0.2	3.93 \pm 0.02	1.6 \pm 0.2
1.07 (cal)	5.5	3.52 (cal)	10.4
0.63	5.8 \pm 0.4	2.88 \pm 0.03	3.9 \pm 0.7
Gates: 4.57–4.78 MeV and 4.88–5.10 MeV		Coincident with 4.20 MeV	
Coincident with 4.68 MeV		2.59 \pm 0.02	2.5 \pm 0.5
3.26 (cal)	4.7	Coincident with 4.36 MeV	
2.12 \pm 0.02	5.7 \pm 1.2	3.06 \pm 0.02	4.0 \pm 1.0
1.93 \pm 0.02	1.8 \pm 0.4	Gates: 2.06–2.27 MeV and 2.32–2.54 MeV	
1.67 \pm 0.02	1.6 \pm 0.2	Coincident with 2.11, 2.14 or 2.16 MeV	
1.51 \pm 0.02	1.2 \pm 0.3	5.72 \pm 0.03	3.9
1.33 \pm 0.02	1.2 \pm 0.4	5.26 \pm 0.02	4.2 \pm 0.5
1.23 \pm 0.02	1.0 \pm 0.4	4.68 (cal)	5.7 \pm 0.9
1.07 (cal)	2.5 \pm 0.4	(3.51 \pm 0.02)	(1.5)
0.63	2.2 \pm 0.4	(2.48 \pm 0.03)	(1.6)
Coincident with 4.62 MeV		2.13 \pm 0.02	2.2 \pm 0.4
2.83 \pm 0.04	0.6 \pm 0.3	1.07 (cal)	
Coincident with 4.93 MeV			
1.86 \pm 0.03	1.5 \pm 0.4		

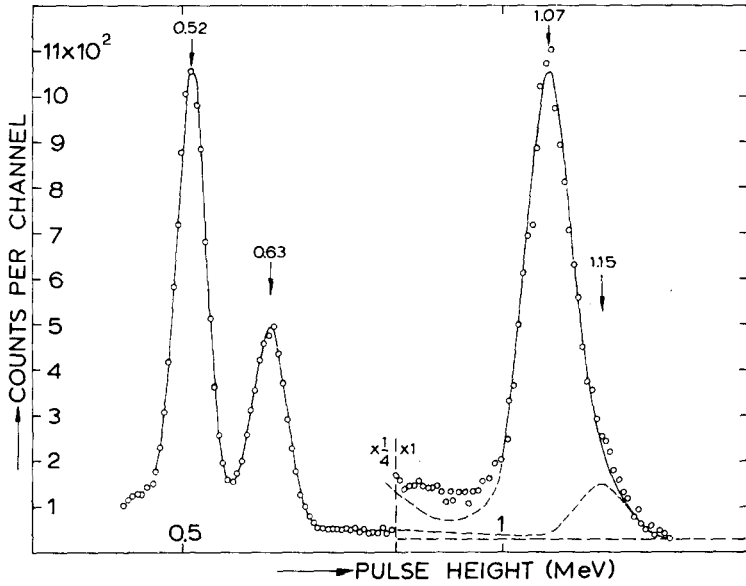


Fig. 5. $^{31}\text{P}(n, \gamma)^{32}\text{P}$ reaction. Spectrum coincident with 6.66–6.87 MeV channel, $\theta = 135^\circ$.

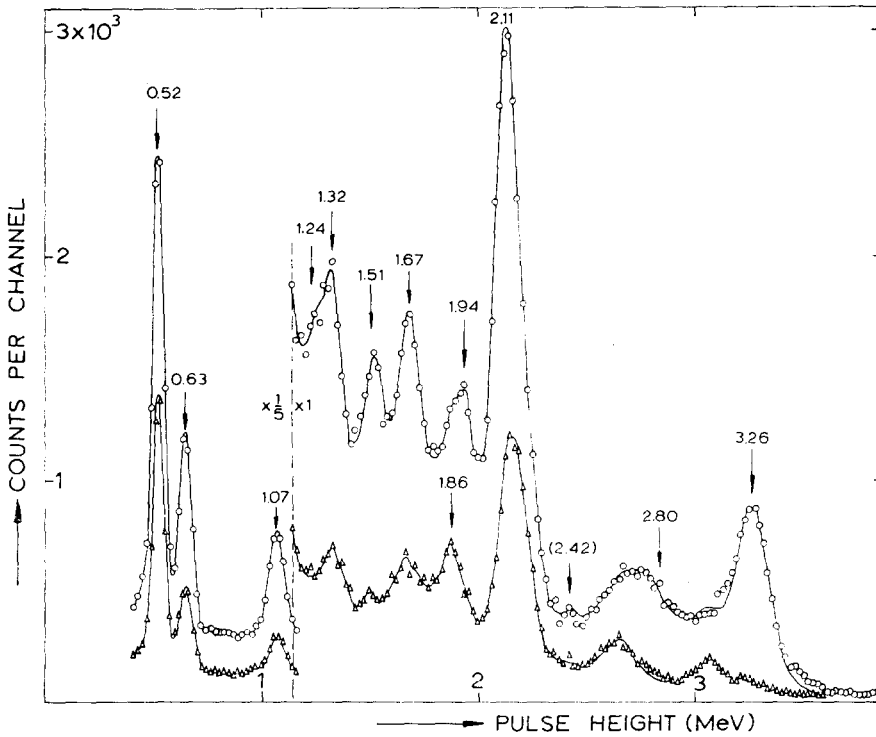


Fig. 6. $^{31}\text{P}(n, \gamma)^{32}\text{P}$ reaction. Spectrum coincident with 4.57–4.78 MeV channel (circles) and spectrum coincident with 4.88–5.10 MeV channel (triangles), $\theta = 135^\circ$.

It should be noticed that the 1.34 and 1.75 MeV gamma rays might be members of cascades through the 1.32 and 1.75 MeV levels, respectively, and thus to the ground state. However, this seems quite improbable from ordinary coincidence measurements, see below. Thus the four weak transitions of 1.34, 1.62, 1.75 and 1.87 MeV all are primaries. The 0.64 MeV gamma ray is due to summing.

Table 3 lists the results of the analysis of four sets of coincidence measurements determining parts a through d of the decay scheme. Both in table 3 and in the figs. 6 and 8–10 only those gamma rays are given which are coincident with gamma rays having a part of their photopeaks in a gate.

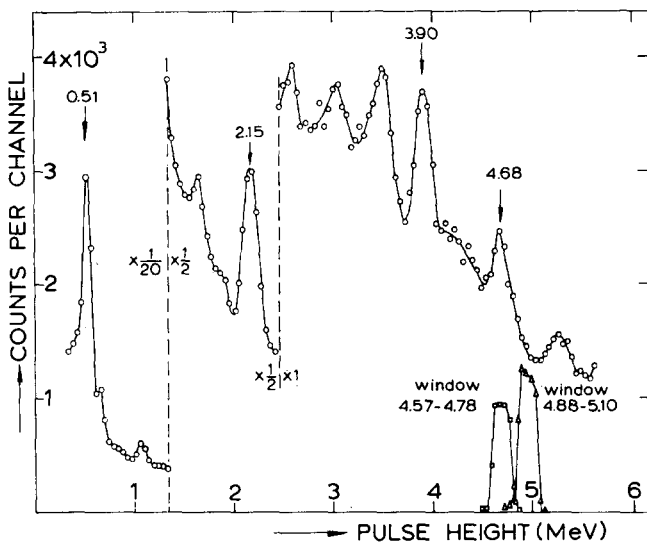


Fig. 7. Single spectrum of the $^{31}\text{P}(n, \gamma)^{32}\text{P}$ reaction measured with D1, with two "self-gated" spectra of $E_\gamma = 4.57\text{--}4.78$ and $E_\gamma = 4.88\text{--}5.10$ MeV.

The spectrum coincident with a 6.66–6.87 MeV gate is shown in fig. 5. This measurement determines part a of the decay scheme. It confirms older measurements ^{9,14}). Moreover a gamma ray of 1.15 MeV is detected, being the ground-state decay of the 1.15 MeV level. The intensities are calculated from the intensity of the 6.79 MeV gamma ray, which is assumed to be 12 % (table 1).

A double coincidence measurement with 4.57–4.78 MeV and 4.88–5.10 MeV gates results in part b of the decay scheme. Both coincidence spectra are given in fig. 6, while fig. 7 demonstrates the self-gating technique in this case. The reference intensity is from tables 1 and 2. In general there often exists uncertainty about the sequence of gamma rays in cascade, since nearly always "mirror" cascades are possible (e.g. the $\text{C} \rightarrow 4.66 \rightarrow 0$ MeV transition is a mirror of the $\text{C} \rightarrow 3.26 \rightarrow 0$ MeV transition). In this case it is possible to determine with high certainty the decay from the angular correlation measurements. Therefore the weak $3.26 \rightarrow 0.08$ MeV transition,

already suggested by the sum-coincidence measurement (a broad 3.26 MeV peak) and by the low-energy tail of the 3.26 MeV line in fig. 6, with an intensity of 0.9% is introduced, see fig. 2. This, and the interpretation of the 2.11 MeV gamma ray is

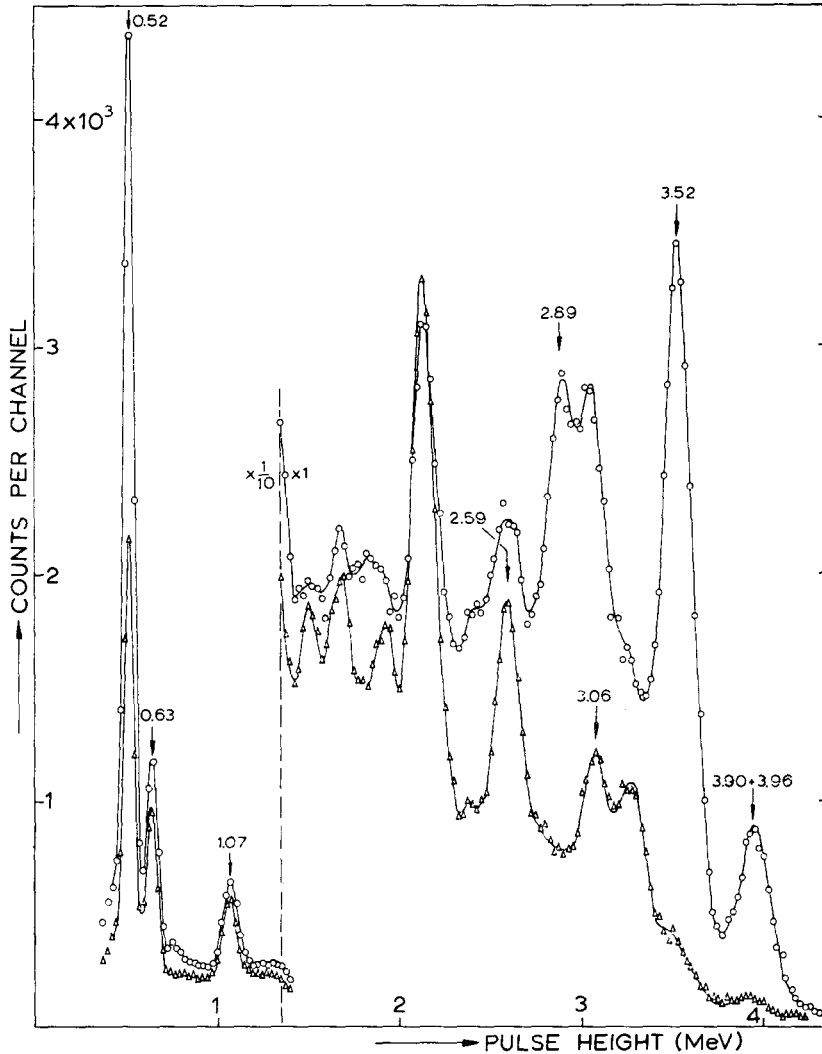


Fig. 8. $^{31}\text{P}(n, \gamma)^{32}\text{P}$ reaction. Spectrum coincident with 3.84–4.05 MeV channel (circles) and spectrum coincident with 4.12–4.33 MeV channel (triangles), $\theta = 135^\circ$.

discussed in the next subsection. The other low-energy gamma rays are fitted in the level scheme using their energies and intensities. A weak 2.42 MeV gamma ray is indicated in fig. 6 which might be the $\text{C} \rightarrow 5.51$ MeV transition. The 5.51 MeV level possibly decays to those at $E_x = 0.52$ and 1.15 MeV.

Part c results from a double coincidence measurement with 3.84–4.05 MeV and 4.12–4.33 MeV gates. The coincidence spectra are shown in fig. 8. An additional coincidence measurement with $E_\gamma = 4.36$ MeV shows a clear 3.06 MeV gamma ray. The intensity of the 3.52 MeV line from table 1 is used as a calibration. The decays through the 4.88 and 5.35 MeV levels are assigned by excluding all other possible mirrors. The broad peak at 3.93 MeV (see also table 2) is a combination of two gamma rays having $E_\gamma = 3.90$ and 3.96 MeV, respectively (note that the weak peak at about this energy in the spectrum coincident with the 4.12–4.33 MeV gate is definitely at a lower energy). A mirror of the $C \rightarrow 4.04 \rightarrow 0.52$ MeV transition through the 4.41 MeV level cannot be excluded definitely.

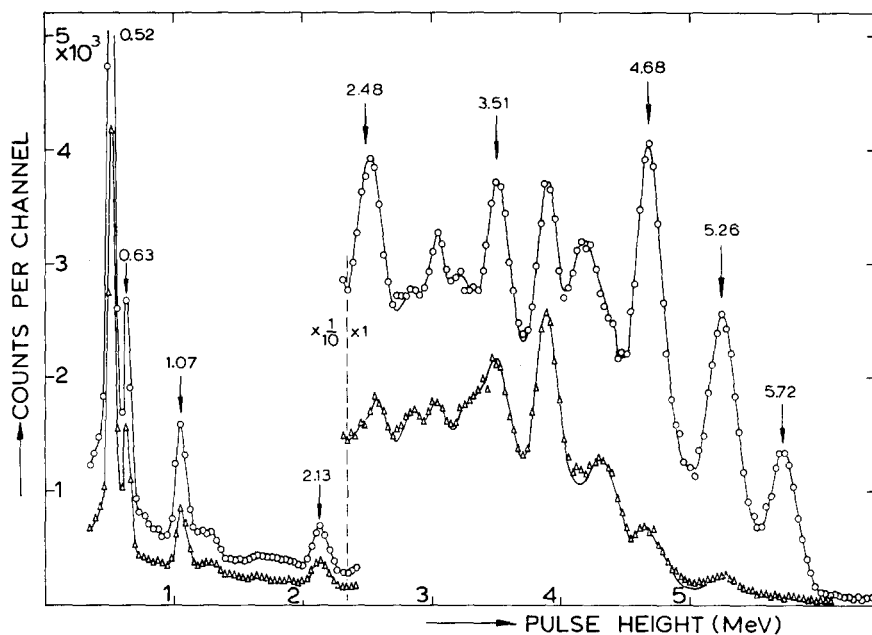


Fig. 9. $^{31}\text{P}(n, \gamma)^{32}\text{P}$ reaction. Spectrum coincident with 2.06–2.27 MeV channel (circles) and spectrum coincident with 2.32–2.54 MeV channel (triangles), $\theta = 135^\circ$.

Part d is the result of a double coincidence measurement with 2.06–2.27 MeV and 2.32–2.54 MeV gates. The spectra are shown in fig. 9. Additional coincidence measurements, extended over 400 channels, were done with the 5.72, 5.26 and 4.68 MeV gamma rays. By comparing the three spectra it can be shown that the following cascades exist: $C \rightarrow 2.22 \rightarrow 0.08$, $C \rightarrow 2.66 \rightarrow 0$, $C \rightarrow 5.78 \rightarrow 0.52$ and $C \rightarrow 3.26 \rightarrow 1.15$ MeV, moreover $C \rightarrow 2.66 \rightarrow 0.08$ or $C \rightarrow 5.35 \rightarrow 0.08$ MeV or a mixture. Thus the broad 2.15 MeV line consists of 2.11, 2.14 and 2.16 MeV gamma rays. The presence of a 2.13 ± 0.02 MeV gamma ray can be understood by inserting the $5.78 \rightarrow 2.22$ and $5.78 \rightarrow 3.26$ MeV transitions. These might be the 3.51 ± 0.02 and 2.49 ± 0.03 MeV gamma rays, respectively.

A double coincidence measurement with 1.02–1.12 MeV and 1.15–1.25 MeV gates confirms the existence of the cascades through the 3.26, 4.04 and 5.35 MeV levels to that at $E_x = 1.15$ MeV.

3.1.2. Spins and parities

Angular correlation measurements were done at three angles $\theta = 90^\circ$, 135° and 180° . The resulting A_2 coefficients are listed in table 4.

TABLE 4
Observed angular correlation coefficients A_2 in the $^{31}\text{P}(\text{n}, \gamma)^{32}\text{P}$ reaction, corrected for solid angle and target size

Cascade (MeV)	A_2^{exp}	Possible spin sequence with $A_2^{\text{theor a)}$
1. C \rightarrow 3.26 \rightarrow 0 ^{b)}	0.093 ± 0.025	$\left\{ \begin{array}{ll} 011 & -0.250 \end{array} \right\}^{\text{e)}$
2. C \rightarrow 3.26 \rightarrow 1.15 ^{b)}	0.18 ± 0.02	$\left\{ \begin{array}{ll} 111 & 0.125 \end{array} \right\}$
3. C \rightarrow 4.04 \rightarrow 1.15 ^{b)}	-0.07 ± 0.05	$\left\{ \begin{array}{ll} 121 & 0.175 \end{array} \right\}$
4. C \rightarrow 5.35 \rightarrow 1.15 ^{b)}	0.21 ± 0.04	
5. C \rightarrow 4.04 \rightarrow 0.08 ^{b)}	0.07 ± 0.03	$\left\{ \begin{array}{ll} 012 & 0.050 \end{array} \right\}^{\text{e)}$
6. C \rightarrow 2.22 \rightarrow 0.08 ^{d)}	0.05 ± 0.01	$\left\{ \begin{array}{ll} 112 & -0.025 \end{array} \right\}$
7. C \rightarrow 1.15 \rightarrow 0.08 ^{d)}	0.02 ± 0.02	$\left\{ \begin{array}{ll} 122 & -0.175 \end{array} \right\}$
8. C \rightarrow 4.04 \rightarrow 0.52 ^{b)}	0.260 ± 0.015	$\left\{ \begin{array}{ll} 010 & 0.500 \end{array} \right\}^{\text{e, e)}$
9. C \rightarrow 4.88 \rightarrow 0.52 ^{b)}	0.34 ± 0.03	$\left\{ \begin{array}{ll} 110 & -0.250 \end{array} \right\}$
10. C \rightarrow 5.78 \rightarrow 0.52 ^{b)}	0.07 ± 0.03	$\left\{ \begin{array}{ll} 120 & -0.250 \end{array} \right\}^{\text{e)}$
11. C \rightarrow 1.15 \rightarrow 0.52 ^{d)}	-0.23 ± 0.02	
12. 3.26 \rightarrow 1.15 \rightarrow 0.52 ^{f)}	0.06 ± 0.04	$\left\{ \begin{array}{ll} 110 & -0.250 \\ 210 & 0.050 \end{array} \right\}$
13. C \rightarrow 3.26 \rightarrow 1.32 ^{b)}	-0.2 ± 0.1	$\left\{ \begin{array}{ll} 121 & 0.175 \\ 122 & -0.175 \\ 123 & 0.050 \end{array} \right\}$

a) Pure dipole transitions assumed, except for the 120 case (second transition pure quadrupole).

b) Initial and final state have even parity, the intermediate state has odd parity. Both γ transitions are assumed to be pure E1.

c) Or any intermediate value, depending on the capturing state spin mixture.

d) Initial, intermediate and final state have even parity. Both γ transitions can be of mixed M1+E2 character. The angular correlation measurement only served to indicate a possible $J \neq 0$ assignment to the intermediate level.

e) Since only the spin sequence 010 has $A_2 > 0.175$ it follows from 8 and 9 that $J(0.52) = 0$. Thus only spin sequences ending on $J = 0$ are taken into account. The 120 sequence cannot be applied to cascade 11 ($J(1.15) = 1$).

f) Initial state has odd parity, the intermediate and final state have even parity. The first transition is assumed to be a pure E1, the second one is a pure M1 transition since $J^\pi(1.15) = 1^+$ and $J^\pi(0.52) = 0^+$.

All intermediate levels, except those at $E_x = 2.22$ and 1.15 MeV have $I_n = 1$ from the (d, p) reaction ^{10, 14}), and thus have odd parity. It is therefore reasonable to expect primary unmixed E1 transitions to these levels. Equally, the decay of odd parity to even parity states is assumed to have pure E1 character.

In principle, the capturing state is an unknown mixture of 0^+ and 1^+ states, with different γ -ray branching percentages. Both states can contribute to the E1 decay to a 1^- level, but E1 transitions to 0^- or 2^- levels can only proceed from the 1^+ state. The I_n values from the (d, p) reaction ^{10, 14}) are used for restricting the possible spin values of the levels.

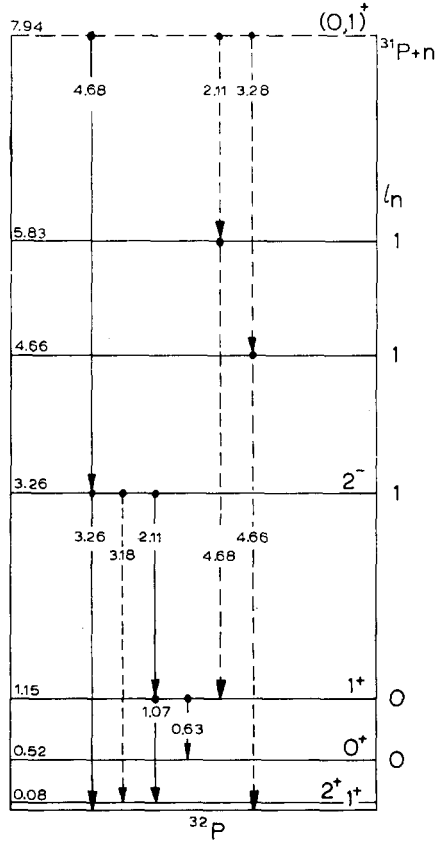


Fig. 10. Part of the ³²P decay scheme, necessary for explaining the anisotropy of the 2.11 and 3.26 MeV γ rays coincident with $E_\gamma \approx 4.68$ MeV. Further discussion see text.

It is known ^{9, 14}) that $J^\pi(1.15) = 1^+$. This spin assignment is confirmed by measurement 11 in table 4. The ground state is characterized by 1^+ also. Thus one expects equal anisotropies for the cascades 1 and 2 in table 4. But actually they differ considerably. For explaining this, one of the cascades might be admixed with another one having a different anisotropy. The three possibilities are given with dotted arrows in fig. 10. Transitions through a mirror of the 1.15 MeV level are not considered since the intensity ratio of the 1.07 and 0.63 MeV gamma rays is about 1 as it should be expected on the basis of the proposed decay scheme (fig. 2). The 4.68 and 2.11 MeV gamma rays in cascade, either the $C \rightarrow 3.26 \rightarrow 1.15$ MeV or the $C \rightarrow 5.83 \rightarrow 1.15$

MeV cascade or a mixture, must occur between states with spin sequence $1 \rightarrow 2 \rightarrow 1$. Only this sequence has, given $J(C) = (0, 1)$ and $J(1.15) = 1$ and assuming pure dipole transitions, a theoretical A_2 coefficient consistent with experiment 2 (table 4). Suppose that only the $C \rightarrow 5.83 \rightarrow 1.15$ MeV cascade exists. The theoretical angular correlation between the first and the third radiation (2.11 and 0.63 MeV, respectively) of the $C \rightarrow 5.83 \rightarrow 1.15 \rightarrow 0.52$ MeV cascade, using $J(0.52) = 0$ (see below), is characterized by $A_2 = 0.175$ (all pure dipole radiation). However, experiment 12 (table 4) gives $A_2 = 0.06 \pm 0.04$, in agreement with a $2 \rightarrow 1 \rightarrow 0$ spin sequence. Thus certainly the $C \rightarrow 3.26 \rightarrow 1.15$ MeV cascade exists, and $J(3.26) = 2$ from measurement 2. Moreover the angular correlation between the first and the third gamma ray of the $C \rightarrow 3.26 \rightarrow 1.15 \rightarrow 0.52$ MeV cascade is found to have $A_2 = 0.19 \pm 0.05$ (not listed in table 4) which agrees with theory, see above. In conclusion, the $C \rightarrow 5.83 \rightarrow 1.15$ MeV cascade does not exist. The low anisotropy of the $C \rightarrow 3.26 \rightarrow 0$ MeV cascade thus must be explained either by an admixture with its mirror cascade through $E_x = 4.66$ MeV or by an admixture of the $3.26 \rightarrow 0.08$ MeV transition. The first case yields $J(4.66) = (0, 1)$, assuming pure dipole radiation and an unknown mixture of both transitions. Suppose that the 3.18 MeV gamma ray (assumed to be E1) is present, then a 25% admixture of this gamma ray to the 3.26 MeV gamma ray is sufficient to explain the A_2 value of measurement 1 in table 4. Since a weak 3.18 MeV line is suggested by the enlarged width of the 3.26 MeV line both in fig. 6 and fig. 4 (table 2), the presence of the 3.18 MeV gamma ray is accepted rather than the $C \rightarrow 4.66 \rightarrow 0$ MeV cascade.

From measurements 8 and 9 (table 4) it is immediately seen that $J(0.52) = 0$, $J(4.04) = 1$ and $J(4.88) = 1$. The assignment $J(4.04) = 1$ is somewhat uncertain, because of the possible mirror cascade through the 4.41 MeV level, but on the other hand it is strengthened by measurements 3 and 5. The A_2 coefficient of experiment 5 is too large, probably due to summing with $E_\gamma = 3.52$ MeV, and the A_2 coefficient in measurement 3 is badly determined. But they both exclude $J(4.04) = 2$, while, on the basis of the decay scheme, $J = 0$ is very improbable. From experiment 4 it follows that $J(5.35) = 2$, while experiment 10 results in $J(5.78) = 1$. The angular correlation 11 rules out $J(1.15) = 0$, and thus $J(1.15) = 1$ (ref. ⁹) from $I_n = 0$ (refs. ^{10, 14}). From 6 it is seen that $J(2.22) \neq 0$. Assuming even parity for the 1.32 MeV level, reasonable because of both the low excitation energy and the relative strong population by the 1.94 MeV gamma ray but in contradiction with Teplov ²¹) ($I_n = 3$), it is seen that $J(1.32) = 2$ from experiment 13; $J = 0$ and $J = 4$ are excluded on the basis of the 1.94 MeV gamma-ray intensity.

It is impossible from measurements 6, 7 and 11 to compute the E2/M1 mixing ratios for the 5.72, 2.14, 6.79 and 1.07 MeV gamma rays, because of the unknown capturing-state spin mixture for each primary transition.

3.2. THE REACTION $^{32}\text{S}(n, \gamma)^{33}\text{S}$

The shell model calculations by Glaudemans ¹⁵) predict the second excited state

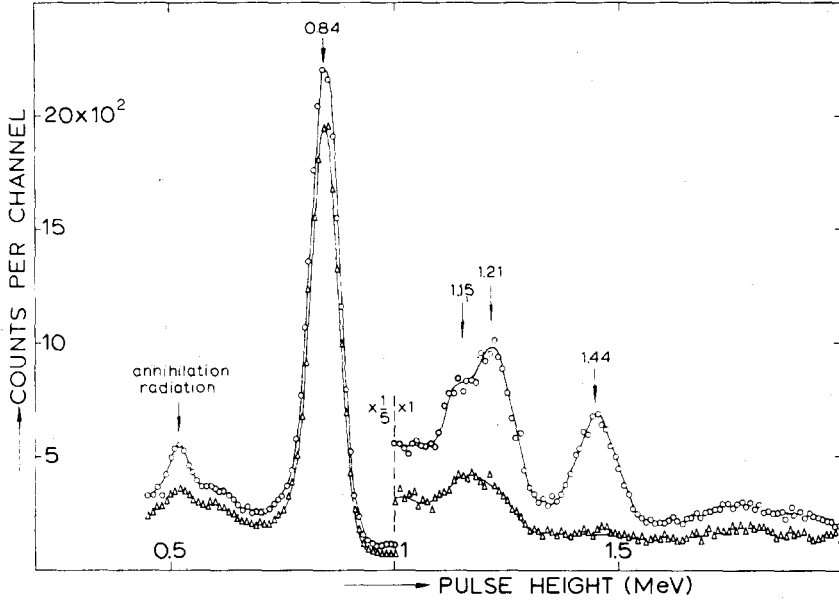


Fig. 11. $^{32}\text{S}(n, \gamma)^{32}\text{S}$ reaction. Spectrum coincident with 7.07–7.33 MeV channel (circles) and spectrum coincident with 7.53–7.78 MeV channel (triangles), $\theta = 135^\circ$, counting time 7.5 d.

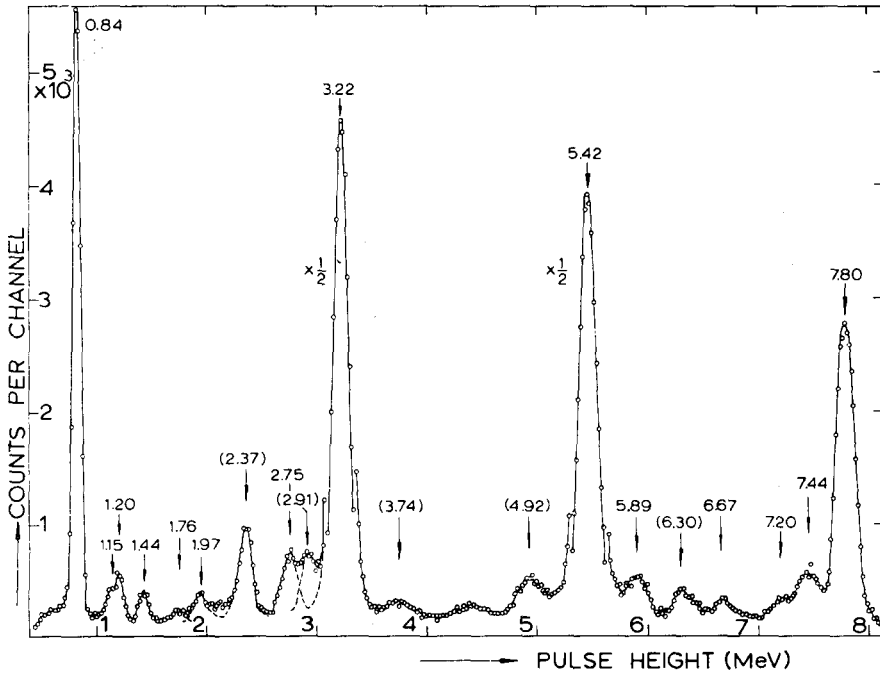


Fig. 12. Sum-coincidence spectrum of the $^{32}\text{S}(n, \gamma)^{32}\text{S}$ reaction. Sum channel 8.53–8.75 MeV, $\theta = 135^\circ$, counting time 65 h.

in the nuclei ^{33}S and ^{33}Cl at an energy of 1.38 MeV with $J^\pi = \frac{5}{2}^+$. In both nuclei the second excited state is found at a much higher energy of 1.97 and 2.1 MeV, respectively. There are reasons to believe that the level at about 1.38 MeV could be missed in the $^{32}\text{S}(\text{d}, \text{p})^{33}\text{S}$ reaction ¹⁵). But a recent investigation ²²) of the $^{32}\text{S}(\text{d}, \text{p}\gamma)^{33}\text{S}$ reaction gives an indication for the existence of a level at 1.34 ± 0.06 MeV decaying through the 0.84 MeV level to the ground state. An investigation of the $^{33}\text{S}(\text{p}, \text{p}')^{33}\text{S}$ reaction yielded a negative result as to the existence of a possible $E_x = 1.4$ MeV state ²³).

From the $^{32}\text{S}(\text{n}, \gamma)^{33}\text{S}$ reaction, having a reaction energy $Q = 8.64$ MeV, gamma rays of 1.52 ± 0.05 (ref. ⁸)) and 7.19 ± 0.03 (ref. ⁴)) or 7.20 ± 0.05 (ref. ¹)) MeV were observed, possibly members of a two-step cascade through a 1.5 MeV level.

The capture cross section ²⁰) of natural sulphur is 0.52 ± 0.02 b. Abundances and cross sections of the other sulphur isotopes indicate that most of the capture occurs in ^{32}S . The most serious contribution (2 %) is from the $^{34}\text{S}(\text{n}, \gamma)^{35}\text{S}$ reaction ¹⁴) having $Q = 6.98$ MeV. The average scattering cross section ²⁰) of natural sulphur is 1.1 ± 0.2 b.

The target consisted of 4 g of sulphur powder compressed in a thin-walled teflon cylinder with inner diam. and length of 1 and 4 cm, respectively.

TABLE 5
Two-step cascades observed in the sum-coincidence spectrum for the reaction $^{32}\text{S}(\text{n}, \gamma)^{33}\text{S}$

Cascade (MeV)	Probable intermediate level (MeV)	Intensity (number of two-step cascades per 100 captures)
0.84 (cal) — 7.80 (cal) (1.15 ± 0.02) ^{b)} — (7.49) ^{c)}	0.84	3.3 ± 0.5 ^{a)} (0.2 ± 0.1)
1.20 ± 0.02 — 7.45 ± 0.04	7.45	0.3 ± 0.1
1.44 ± 0.01 — 7.20 ± 0.04	(7.19)	0.27 ± 0.05
1.76 ± 0.03 — 6.88 ^{c)}	6.89	0.14 ± 0.05
1.95 ± 0.02 — 6.68 ± 0.03	1.97	0.3 ± 0.1
2.75 ± 0.03 — 5.89 ± 0.04	5.89	1.1 ± 0.3
3.22 (cal) — 5.42 (cal)	3.22	20 ^{d)}

^{a)} Corrected for summing.

^{b)} Might be the $1.16 \rightarrow 0$ MeV transition in ^{36}Cl . The intensity corresponds to a 0.02 % chlorine contamination of the sulphur.

^{c)} Energy calculated.

^{d)} From ref. ¹⁴). A 20 % error might exist in this value. This error is not included in the calculations.

The spectra coincident with 7.07–7.33 MeV and 7.53–7.78 MeV gates are shown in fig. 11. Gamma rays are seen at $E_\gamma = 0.84$, 1.15 ± 0.03 , 1.21 ± 0.02 and 1.44 ± 0.01 MeV, the first being the $0.84 \rightarrow 0$ MeV transition. The background at $E_\gamma > 1.60$ MeV is due to pile-up of pulses in the stationary counter. Fig. 12 gives a sum-coincidence spectrum; the results are listed in table 5. The peaks at 2.37 ± 0.02 , 2.91 ± 0.03 and

4.92 ± 0.04 MeV are probably due to summing although their intensities seem rather high. Fig. 13 gives that part of the decay scheme relevant to the present measurements. In both figs. 11 and 12 a clear peak at 1.44 ± 0.01 MeV is seen. It is verified, by varying the detector solid angle, that this gamma ray is not due to summing in either of the detectors. The intensity, derived from the sum-coincidence measurement, is 0.27 ± 0.05 %, assuming 20 % intensity ¹⁴⁾ for the 3.22 MeV gamma ray.

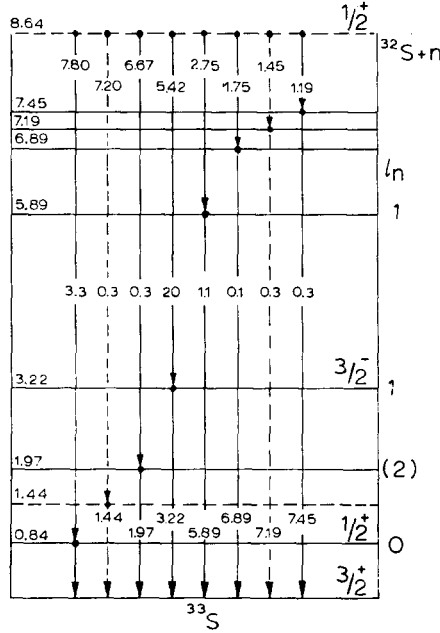


Fig. 13. Two-step cascades in the $^{32}\text{S}(n, \gamma)^{32}\text{S}$ reaction. The energy levels, I_n values and J values are from ref. ¹⁴⁾. The intensities are in number of gamma rays per 100 captures.

In coincidence with $E_\gamma = 1.44$ MeV a 7.20 ± 0.04 MeV gamma ray is found, but no cascades exciting a possible 1.44 MeV level could be identified.

Angular correlation measurements, using five angles, show a non-isotropic distribution of the 1.44 MeV gamma ray. A least-squares fit yields either $A_2 = -0.080 \pm 0.031$ and $A_4 = 0.025 \pm 0.042$ ($\chi^2 = 0.62$) or $A_2 = -0.072 \pm 0.025$ and $A_4 \equiv 0$ ($\chi^2 = 0.49$). The χ^2 has been normalized by dividing through the number of free parameters. The second result is used. It is immediately seen that spin and parity of the intermediate state $J^\pi = \frac{1}{2}^\pm$ ($A_2 = 0$) and $J^\pi = \frac{3}{2}^-$ ($A_2 = -0.20$; $J^\pi(C) = \frac{1}{2}^+$, $J^\pi(0) = \frac{3}{2}^+$ and pure E1 radiation assumed) are excluded. One can also exclude $J^\pi = \frac{5}{2}^-$, taking into account any M2-E3 mixing in the primary transition if the second transition is assumed to be pure E1. Thus there remains $J^\pi = \frac{3}{2}^+$ or $\frac{5}{2}^+$. The primary gamma ray then is either a M1/E2 or a pure E2 transition.

A comparison with the intensity of the $C \rightarrow 0.84$ MeV M1 transition, about 3 %,

shows that if the 1.44 MeV gamma ray is a M1 primary it is about 10 times faster than the $C \rightarrow 0.84$ transition. Although it seems not improbable that the 7.20 MeV gamma ray is a primary, it cannot be proved by these arguments.

4. Discussion

4.1. THE REACTION $^{31}\text{P}(n, \gamma)^{32}\text{P}$

The gamma-ray energies and intensities in table 1 are in fair agreement with the compilation given in ref. ¹⁴). The decay scheme (see fig. 2) is with respect to the strong de-excitation modes in good agreement with that proposed by Groshev *et al.* ¹) and as verified by Manning and Bartholomew ⁹). More information is obtained now about the decay of low-lying levels, explaining a part of the low-energy gamma rays.

The spin assignments to the 1.15 and 3.26 MeV levels, $J = 1$ and 2, respectively, are in agreement with the assignments of Manning and Bartholomew ⁹). It must be mentioned that in ref. ⁹) for the $C \rightarrow 3.26 \rightarrow 0$ MeV cascade an anisotropy $A_2 = 0.19 \pm 0.03$ is given. This high value (cf. table 4) is probably due to summing in which case the strongly anisotropic 3.52 MeV gamma ray appears in the spectrum. This is prevented in the present experiment by taking a narrow window on $E_\gamma = 4.68$ MeV. The $J(2.22) \neq 0$ assignment is consistent with Holtebekk's assignment $J^\pi(2.22) = 1^+$. The spin assignments to the 0.52 and 1.32 MeV levels, $J = 0$ and (2), respectively, agree with shell model calculations ¹⁵).

Sometimes the reduced gamma-ray intensities of primaries are used to determine the character (electric or magnetic) of these gamma rays. In ref. ²⁴) a criterion is introduced according to which it is possible to show that some primaries are E1 transitions. This criterion is not used in the present investigation because the parities of all levels under consideration are known. Nevertheless it is of some value to investigate a little closer the radiation strengths of E1 primaries.

This E1 radiation strength is defined by ²⁵)

$$k_{\text{E1}} = \frac{\Gamma'_\gamma(\text{E1})_{\text{obs}}}{E^3 A^{\frac{2}{3}} D},$$

in which A is the nuclear mass number, D the average spacing of levels near the capturing state with the same spin and parity as this state and $\Gamma'_\gamma(\text{E1})_{\text{obs}}$ is the observed partial radiation width for a particular E1 gamma ray with energy E . The total radiation width Γ_γ of the capturing state, which is not a level, is defined as the weighted mean value of the radiation widths of contributing s-wave resonances. The theoretical expression for the partial radiation width, neglecting the statistical factor, is ^{25, 26}) $\Gamma'_\gamma(\text{E1}) = 0.11 E^3 A^{\frac{2}{3}} D/D_0$ in which $\Gamma'_\gamma(\text{E1})$ is in eV and E , D and D_0 in MeV. The numerical constant is calculated using the nuclear radius $R = 1.5 A^{\frac{1}{3}}$ fm. The quantity D_0 is the spacing of single particle levels with equal spin and parity which is approximately 15 MeV, a value which is used in the following.

The mean value of k_{E1} for known E1 gamma rays is ²⁵⁾ $3 \times 10^{-3} \text{ eV} \cdot \text{MeV}^{-4}$ while the theoretical expression yields $7.3 \times 10^{-3} \text{ eV} \cdot \text{MeV}^{-4}$.

In ref. ²⁴⁾ a gamma ray is said to be an E1 if $k = k_{E1} > 3 \times 10^{-3} \text{ eV} \cdot \text{MeV}^{-4}$ because the mean value of k for known M1 gamma rays is $k = 3 \times 10^{-4} \text{ eV} \cdot \text{MeV}^{-4}$ and the supposed strength distribution of M1 radiation effectively excludes values larger than $3 \times 10^{-3} \text{ eV} \cdot \text{MeV}^{-4}$.

TABLE 6
Primary E1 radiation strengths in the $^{31}\text{P}(n, \gamma)^{32}\text{P}$ reaction

E_γ (MeV)	$k_{E1} \times 10^3 (\text{eV} \cdot \text{MeV}^{-4})$	E_γ (MeV)	$k_{E1} \times 10^3 (\text{eV} \cdot \text{MeV}^{-4})$
4.68	0.9	2.59	1.0
3.90	2.6	2.16	4.2
3.06	1.7		

The calculated k_{E1} values for five primary E1 gamma rays are listed in table 6. In the calculations $\Gamma_\gamma = 0.5 \text{ eV}$, estimated from the widths in neighbouring light nuclei (^{27,28}), and $D = 0.05 \text{ MeV}$, from Cameron's inspection ²⁹⁾ of s-wave resonance data given in ref. ²⁰⁾, are used if both $J(C) = 0$ and 1 can contribute to the transition. In cases in which only $J(C) = 1$ can contribute $D = 0.07 \text{ MeV}$ is used, because from statistical considerations one expects the number of levels with spin J to be proportional to $2J+1$.

In conclusion, only the 2.16 MeV gamma ray obeys the criterion. The other k_{E1} values are close to the experimental mean value of $3 \times 10^{-3} \text{ eV} \cdot \text{MeV}^{-4}$.

4.2. THE REACTION $^{32}\text{S}(n, \gamma)^{33}\text{S}$

The decay of a possible level ²²⁾ at $E_x = 1.34 \text{ MeV}$ through the $E_x = 0.84 \text{ MeV}$ state could not be detected in the present experiment since the two gamma rays involved in this decay are covered by the annihilation radiation and by the strong 0.84 MeV line due to the $C \rightarrow 0.84 \rightarrow 0 \text{ MeV}$ cascade.

The sum-coincidence measurement confirms the existence of two-step cascades through ¹³⁾ $E_x = 0.84, 1.97, 3.22$ and 7.42 MeV , the latter with slightly different energy. The observed 1.44–7.20 MeV cascade might be the one assumed by Burmistrov ¹³⁾ to proceed through $E_x = 7.02 \text{ MeV}$. A decay through $E_x = 4.05 \text{ MeV}$ (ref. ¹³⁾) was not observed here, while the cascades through $E_x = 5.89$ and 6.89 MeV were not seen earlier.

We are indebted to Professor P. M. Endt for his continuous interest in this work and to Dr. H. Postma for his fruitful help. We thank Mr. H. Gruppelaar, especially for his careful analysis of the pulse-height distributions of mono-energetic gamma rays and Mr. E. Kools for his indispensable technical assistance. One of us (P.S.) likes to thank the Foundation F.O.M. for a scholarship.

This investigation was partly supported by the joint programme of the "Stichting voor Fundamenteel Onderzoek der Materie" and the "Nederlandse Organisatie voor Zuiver Wetenschappelijk Onderzoek". The hospitality and co-operation of the "Stichting Reactor Centrum Nederland" were highly appreciated.

References

- 1) L. V. Groshev, A. M. Demidov, V. N. Lutsenko and V. I. Pelekhov, Atlas of gamma-ray spectra from radiative capture of thermal neutrons (Pergamon, London, 1959)
- 2) L. V. Groshev, A. M. Demidov, V. N. Lutsenko and A. Malov, *Izv. Akad. Nauk (ser. fiz.)* **24** (1960) 791
- 3) H. T. Motz, R. E. Carter and W. D. Barfield, Pile neutron research in physics (IAEA, Vienna, 1962) p. 225
- 4) G. A. Bartholomew and L. A. Higgs, Chalk River Report AECL No. 669 (1958)
- 5) J. W. Knowles, *Can. J. Phys.* **37** (1959) 203
- 6) A. M. Hoogenboom, *Nucl. Instr.* **3** (1958) 57
- 7) B. B. Kinsey, G. A. Bartholomew and R. L. Walker, *Phys. Rev.* **85** (1952) 1012
- 8) T. H. Braid, *Phys. Rev.* **102** (1956) 1109
- 9) G. Manning and G. A. Bartholomew, *Phys. Rev.* **115** (1959) 401
- 10) T. Holtebekk, *Nuclear Physics* **37** (1962) 353
- 11) G. Trumpy, Joint Establishment for Nuclear Energy Research Report JENER No. 13 (1957)
- 12) J. F. Vervier, *Nuclear Physics* **26** (1961) 10
- 13) V. R. Burmistrov, *Izv. Akad. Nauk (ser. fiz.)* **23** (1959) 898
- 14) P. M. Endt and C. van der Leun, *Nuclear Physics* **34** (1962) 1
- 15) P. W. M. Glaudemans, Thesis, Utrecht (1964)
- 16) B. N. Brockhouse, *Rev. Sci. Instr.* **30** (1959) 136
- 17) H. Bjerrum Møller, F. J. Shore and V. L. Sailor, *Rev. Sci. Instr.* **32** (1961) 654
- 18) H. de Waard, *Nucleonis* **13**, no. 7 (1955) 36
- 19) A. M. Feingold and S. Frankel, *Phys. Rev.* **97** (1955) 1025
- 20) D. J. Hughes and R. B. Schwartz, Neutron Cross Sections, BNL-325 (1958) 2nd ed.
- 21) I. B. Teplov, *JETP (Soviet Physics)* **4** (1957) 31
- 22) J. M. O'Dell and F. W. Prosser, *Bull. Am. Phys. Soc.* **9** (1964) 667 and private communication
- 23) C. van der Leun and P. M. Endt, *Nuclear Physics* **53** (1964) 540
- 24) G. A. Bartholomew and J. F. Vervier, *Nuclear Physics* **50** (1964) 209
- 25) G. A. Bartholomew, *Ann. Rev. Nucl. Sci.* **11** (1961) 259
- 26) J. M. Blatt and V. F. Weisskopf, Theoretical nuclear physics (John Wiley and Sons, New York, 1952)
- 27) J. S. Levin and D. J. Hughes, *Phys. Rev.* **101** (1956) 1328
- 28) A. Stolovy and J. A. Harvey, *Phys. Rev.* **108** (1957) 353
- 29) A. G. W. Cameron, *Can. J. Phys.* **36** (1958) 1040